RSC Advances

This article can be cited before page numbers have been issued, to do this please use: M. Moghadam, M. Zakeri, V. Mirkhani, S. Tangestaninejad, I. Mohammadpoor-Baltork and Z. Pahlevanneshan, *RSC Adv.*, 2016, DOI: 10.1039/C6RA16704G.

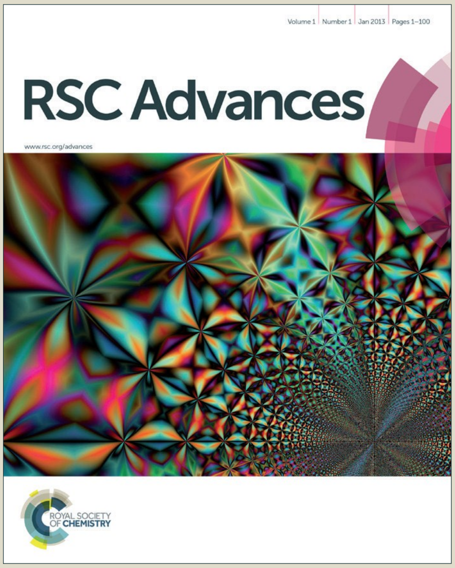

ROYAL SOCIETY OF CHEMISTRY

www.rsc.org/advances

View Article Online
DOI: 10.1039/C6RA16704G

Journal Name
RSCPublishing

sCite this: DOI: 10.1039/x0xx00000x

Received 00th January 2012,
Accepted 00th January 2012

DOI: 10.1039/x0xx00000x

www.rsc.org/

Synthesis and characterization of a host (A new thiol based dendritic polymer)-guest (Pd nanoparticles) nanocomposite material: An efficient and reusable catalyst for C–C coupling reactions

Maryam Zakeri, Majid Moghadam,* Valiollah Mirkhani,* Shahram Tangestaninejad, Iraj Mohammadpoor−Baltork, Zari Pahlevanneshan

The catalytic activity of a new thiol based dendritic polymer immobilized on nano silica containing palladium nanoparticles was studied in C-C coupling reactions. In this manner, functionalized silica nanoparticles were reacted with 1,3,5-benzenetricarbonyl and then with 1,2-ethanedithiol. Finally, this new dendritic material was used as host for carrying of Pd nanoparticles. Thermogravimetric and elemental analyses are in a proper correlation and confirm the successful synthesis of the dendritic polymer. The characterization of the catalyst by transmission electron microscopy, EDX and elemental mapping, show a uniform dispersed, nano−scaled Pd particles in denderimer's cavities and also on the surface functional groups. This insoluble nanosilica thiolated dendritic polymer-supported Pd nanoparticles, showed a set of favorable properties to be used as a heterogeneous and reusable catalyst in the Suzuki−Miyaura and Heck C-C coupling reactions.

Introduction

Dendrimers are a group of nanosized, three dimensional polymers and a class of macromolecules having highly branched architecture.[1] This family of polymers is considered as one of the best synthetic molecules, which suggest perfect properties, such as high degree of branching units, high density of facial functional group, nanosized scale, internal cavities and also high ability of monodispersion of metallic nanoparticles.[2−5]
Due to these specific characteristics, dendrimers have potential applications in various high technologies, such as pharmaceutical, biomedical and industrial uses.[6, 7]
Dendrimers are synthesized by stepwise growth from core to first and second or maybe more generations,[8] thus designing a new dendrimer with new interior and surface functional groups is a tricky and challenging issue. Dendrimer bearing higher generations are almost spherical and the cavities inside the dendrimers are approximately in the range of nanometer,[9, 10] which can be used as a host for encapsulation of nanoparticles, mostly transition metals, such as Pd,[11−13] Cu,[14−16] Au,[17−19] Ag,[20] Pt,[21, 22] and Ru.[23, 24]
Multiple internal and external functional groups enable the dendrimer to act as proper host for a various range of ions and molecules. These functional groups can easily act as a stabilizer for the encapsulated particles by different methods such as covalent bond formation, electrostatic interactions, hydrogen bonding and etc.[9,25]
Palladium nanoparticles (Pd−NPs), consisting of only several or tens of atoms, are novel catalytic materials, also have a number of other applications, including hydrogen storage,[26] sensing,[27] coatings, polymer membranes,[28] and fuel cells.[29]
Pd nanoparticles are excellent catalysts for hydrogenation,[30] dehydrogenation[31] and also coupling reactions such as carbon−carbon,[32] carbon−sulfur[33] and carbon–nitrogen.[34]
The recovery and reusability of this precious metal catalyst represent a key issue for the sustainable development of any catalytic applications. For this purpose, palladium nanoparticles have been supported by a variety of conventional and non−conventional supports, such as, polymers,[35−38] metal−organic frameworks,[39] anthracene derivatives,[40] ion exchange resins,[41] ligands,[42] surfactants,[43,44] and dendrimers.[45,46] The strong interactions between the palladium and soft sulfur based donors, make sulfur−containing supports highly efficient stabilizers for nanoparticles.[47−49] The size and morphology of the resulting palladium nanoparticles depend on several different reaction conditions. These conditions include the surfactant used, the type and amount of reducing agent employed, the reaction time and the properties of stabilizing agent.[50, 51]
In continuation of our previous works on the application of dendritic-based catalysts in organic synthesis,[11,14,52-57], here we wish to report the synthesis of a host (a new thiol based dendritic polymer)-guest (Pd nanoparticles) nanocomposite material and its application as catalyst for the Suzuki–Miyaura and Heck C-C coupling reactions (Scheme 1).

Department of Chemistry, Catalysis Division, University of Isfahan, Isfahan, 81746–73441 (Iran) Fax: +98–31–36689732; Tel: +98–31–37934920. E–mail: moghadamm@sci.ui.ac.ir, mirkhani@sci.ui.ac.ir

View Article Online
DOI: 10.1039/C6RA16704G

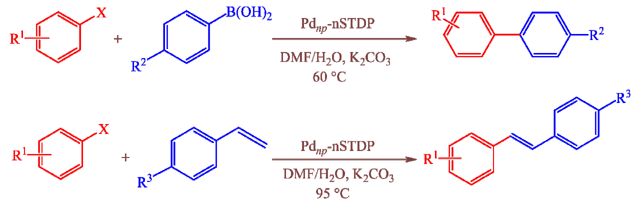

Scheme 1. Suzuki–Miyaura cross–coupling and Heck reactions catalyzed by Pd$_{np}$–nSTDP

Experimental

Materials and reagents

All commercially available reagent grade chemicals were purchased from Merck, Fluka and Sigma–Aldrich. All reagents and solvents were used without further purification. FT–IR spectra were recorded on a Jasco 6300D instrument in the range of 400–4000 cm^{-1}. Thermal gravimetric analysis (TGA) was recorded on a Mettler TG50, under air flow at a consistent heating of 5 °C min^{-1} in the range of 0-600 °C. Elemental analysis was obtained on LECO CHNS–932 analyzer. The X–ray photo–electron spectroscopy (XPS) measurements were performed on XPS–Auger Perkin Elmer 8025-BesTec electron spectrometer, using a Gammadata–scienta ESCA200 hemispherical analyzer equipped with an Al (Kα = 1486.6 eV) X–ray source. The Pd content of the catalyst was measured by an inductively coupled plasma optical emission spectrometry (ICP–OES), via a Jarrell–Ash 1100 ICP analyzer. Scanning electron microscopy images were performed on a Hitachi S–4700 field emission–scanning electron microscope (FE–SEM). Transmission electron microscopy (TEM) measurements were carried out on a Philips CM10 analyzer operating at 100 kV. Substances were identified and quantified by gas chromatography (GC) on an Agilent GC 6890 equipped with a 19096C006 80/100 WHP packed column and a flame ionization detector (FID). In GC experiments anisole was used as internal standard.

The procedure for the preparation of nanosilica thiolated dendritic polymer-supported Pd particles (Pd$_{np}$–nSTDP) was as follows:

Propylthiol–Functionalized Nano–Silica (PT–nSiO$_2$)

(3–Mercaptopropyl)trimethoxysilane (8.5 mL) was added dropwise via a syringe to a stirred solution of activated nano–silica (3 g) in dried toluene (50 mL) under reflux conditions for 12 h. The reaction medium was cooled to room temperature and filtered. The solid was washed overnight with dried toluene by soxhlet extractor to remove the unreacted starting materials. The white solid was dried in a vacuum oven at 110 °C.

BCC1–nSiO$_2$

To a solution of 1,3,5–benzenetricarbonyl trichloride (2.65 g, 10 mmol) and diisopropylethylamine (DIPEA) (10 mmol, 1.7 mL) in anhydrous THF (10 mL) was slowly added the previously synthesized PT–nSiO$_2$ (2 g).The reaction mixture was cooled to 0 °C and stirred overnight. The solid material was filtered, washed overnight with hot tetrahydrofuran (THF) in a Soxhlet extractor. Then dried in a vacuum oven at 60 °C.

Nano–Silica Supported Thiolated Dendritic Polymer (G1)

BCC1–nSiO$_2$ (1 g) in dimethylformamide (DMF) (12 mL) was treated with 1,2–ethanedithiol (8.11 mmol, 0.7 mL) and DIPEA (8 mmol, 1.4 mL) at 80 °C for 16 h. The solid material was filtered and washed overnight with hot ethanol in a Soxhlet extractor and dried in a vacuum oven at 60 °C.

BCC2–nSiO$_2$

G1 (1 g) was added slowly to a solution of 1,3,5–benzenetricarbonyl trichloride (2.4 g, 9 mmol) and DIPEA (9 mmol, 1.55 mL) in THF (20 mL). The reaction mixture was cooled and stirred at 0 °C for 16 h. The reaction mixture was filtered and the solid was washed overnight with hot THF in a Soxhlet extractor. The BCC2–nSiO$_2$ was dried in a vacuum oven at 60 °C.

Nano–Silica Supported Thiolated Dendritic Polymer (G2 or nSTDP)

To a solution of BCC2–nSiO$_2$ (1 g) in DMF (20 mL), 1,2–ethanedithiol (9.5 mmol, 0.8 mL) and DIPEA (9.5 mmol, 1.65 mL) were added slowly and the reaction mixture was stirred at 80 °C for 16 h. The resulting nano–silica supported dendritic polymer (G2 or nSTDP) was filtered and washed with hot ethanol overnight in a Soxhlet extractor and dried in a vacuum oven at 60 °C.

Nano–Silica Thiolated Dendritic Polymer Supported Palladium Nanoparticles (Pd$_{np}$–nSTDP)

Initially, Na$_2$PdCl$_4$ solution was prepared by mixing and dissolving of PdCl$_2$ (240 mg, 1.36 mmol) and NaCl (176 mg, 3 mmol) in methanol (10 mL), under stirring at room temperature for 24 h and then filtered. Methanol (40 mL) and nSTDP (1 g) was added to this solution. The slurry was then stirred at 60 °C for 24 h. After cooling the mixture to room temperature, sodium acetate (0.76 g, 9.28 mmol) was added and stirred for 1 h. The solid was filtered, washed with methanol, water and acetone continuously, to remove the unreacted precursors, and finally dried in vacuum and Pd$_{np}$–nSTDP catalyst (1.09 g) as a dark brown solid was prepared. Palladium analysis (ICP): 0.14 mmol Pd/ g catalyst. Average particle diameter: 3.6 ± 0.5 nm (based on TEM and particle size analyses).

Typical Procedure for Suzuki–Miyaura Cross–Coupling Catalyzed by Pd$_{np}$–nSTDP

Aryl halide (1 mmol), phenylboronic acid (1.1 mmol), K$_2$CO$_3$ (1.5 mmol) and the Pd$_{np}$–nSTDP catalyst (5 mg, 0.07 mol%) were added to 3 ml of DMF/H$_2$O (2:1). The reaction mixture was stirred at desired temperature under air atmosphere. The results are summarized in Table 3. The yields were quantified by GC analysis. After the end point, the solution was filtered and the products were extracted with ethyl acetate (3×10 mL).

DOI: 10.1039/C6RA16704G

The organic phase was washed with water (2×10 mL), dried over anhydrous Na_2SO_4 and concentrated in vacuum to afford the pure product.

Typical Procedure for Heck Reaction Catalyzed by Pd_{np}−nSTDP

Aryl halide (1 mmol), styrene (1.1 mmol), K_2CO_3 (1.5 mmol) and Pd_{np}−nSTDP (10 mg, 0.14 mol% Pd) were added in 3 mL of DMF/H_2O (1:2). The reaction mixture was stirred at 95 °C under an air atmosphere for desired time summarized in Table 5. The progress of the reaction was tracked by GC. After completion, the reaction mixture was cooled, poured in water and extracted by diethyl ether (2×10 mL). The organic phase was washed with water (3×10 mL) and dried over anhydrous $MgSO_4$. After evaporation of the solvent the pure product was afforded.

Results and discussion

Preparation and characterization of nanosilica thiolated dendritic polymer-supported Pd particles (Pd_{np}−nSTDP)

The first step for the synthesis of nanosilica thiolated dendritic polymer was modification of the activated nanosilica with (3−mercaptopropyl)trimethoxysilane, to obtain the thiol functionalized nanosilica (PT−$nSiO_2$).[58] The addition of 1,3,5-benzenetricarbonyl trichloride (BCC) to the surface−attached propylthiol nanosilica was carried out at 0 °C, to substitute only one of the chlorine atoms to achieve BCC1−$nSiO_2$. In the next step, BCC1−$nSiO_2$ was thiolated via addition of 1,2−ethanedithiol to prepare G1. The G2 was achieved by addition of 1,3,5-benzenetricarbonyl trichloride and 1,2−ethanedithiol, successively (Scheme 2).

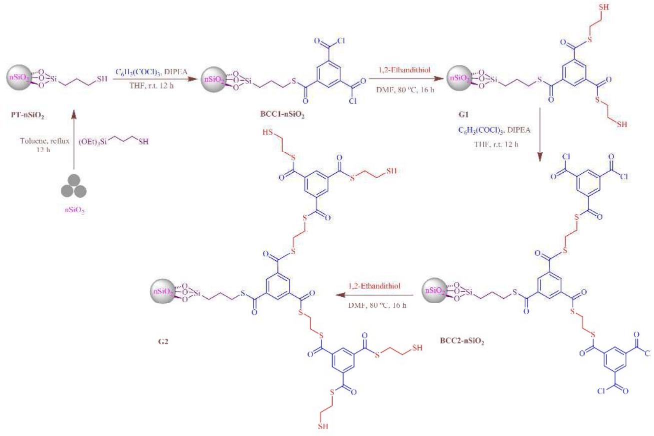

Scheme 2. Synthesis of nano−silica Thiolated dendritic polymer (G2 or nSTDP).

Synthesis of dendritic polymer was step by step monitored by FT−IR spectroscopy, TGA and also elemental analysis. FT-IR spectra were recorded neat and only significant absorption in cm^{-1} are indicated. The FT−IR spectrum of PT−$nSiO_2$ (Fig. 1a) showed a broad O─H stretching band at 3200–3400 cm^{-1} and a strong Si─O─Si stretching band about 1000 –1100 cm^{-1}. Also, the characteristic bands for C─H_{aliph} appear at 1450 and 2950 cm^{-1}.[11] In the FT−IR spectra of BCC1−$nSiO_2$, G1, BCC2−$nSiO_2$ and G2 (Fig. 1b–e), in addition to the above mentioned vibrations, the bands at 1690–1710 cm^{-1} (C=O) is a good indication for the presence of carbonyl groups on the nano−silica.[59]

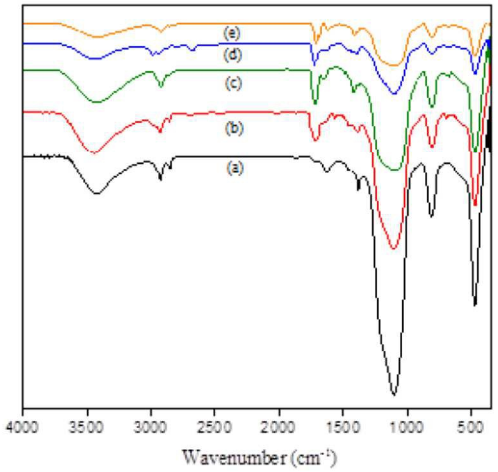

Fig. 1. FT-IR spectrum of: a) PT−$nSiO_2$, b) BCC1− $nSiO_2$, c) G1, d) BCC2−$nSiO_2$ and e) G2

The TGA survey scan was run at 5 °C per minute. The TGA curve of PT−$nSiO_2$, BCC1−$nSiO_2$, G1, BCC2−$nSiO_2$ and G2, over the temperature range from 0 to 600 °C shows a double steps descending, which indicates a weight loss occurred. The first step is due to loss of residual water in the porous sample and the second step reflects the removal of organic moieties on the surface. The TGA features are imaged in Figure 2.

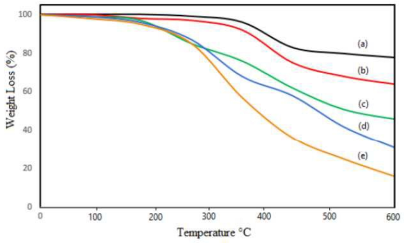

Fig. 2. TGA spectra of: a) PT−$nSiO_2$; b) BCC1−$nSiO_2$; c) G1; d) BCC2−$nSiO_2$ and e) G2 (nSTDP)

Elemental analysis calculation is in a good relevance with TGA data (Table 1).[60] The elemental analysis results for sulfur content showed a decrease from PT−$nSiO_2$ to BCC1−$nSiO_2$ and also from G1 to BCC2−$nSiO_2$ due to addition of 1,3,5-benzenetricarbonyl trichloride. Consequently, this amount increased via further addition of 1,2−ethanedithiol. As it is shown in Table 1, the nitrogen content was also investigated. The presence of nitrogen in the CHNS is due to utilization of DIPEA as a base trapped in the pores of nanosilica.

View Article Online
DOI: 10.1039/C6RA16704G

Table 1. TGA and elemental analysis (EA) results for the synthesis of nano−silica thiolated dendritic material

		C	H	N	S	O	Cl	Total
PT−nSiO$_2$	TGA (wt%)	10.20	1.98	−	9.07	−	−	21.26
	EA (wt%)	10.04	1.96	−	9.01	−	−	21.01
BCC1−nSiO$_2$	TGA (wt%)	16.61	1.03	−	3.69	6.23	8.07	35.65
	EA (wt%)	17.81	1.08	1.72	3.72	−	−	24.36
G1	TGA (wt%)	28.32	2.80	−	14.16	7.96	−	53.26
	EA (wt%)	29.66	2.93	0.38	14.83	−	−	47.81
BCC2−nSiO$_2$	TGA (wt%)	31.49	1.77	−	12.35	12.50	10.80	68.92
	EA (wt%)	32.21	1.97	1.43	12.94	−	−	48.55
G2	TGA (wt%)	37.81	3.22	−	31.21	12.15	−	84.41
	EA (wt%)	39.17	3.85	0.25	32.19	−	−	75.46

After synthesis and characterization of nSTDP, the dendritic polymer was used as host for carrying the palladium nanoparticles. The supported Pd nanoparticles were obtained by the reaction of Na_2PdCl_4 with nSTDP in the presence of sodium acetate as reducing agent (Scheme 3).[61] As mentioned in the literature, the Pd nanoparticles can be trapped by the cavities and also by the surface functional groups.[25] Based on three dimensional structure of dendrimers, internal sulfides and oxygenes, and also external thiol groups of this dendritic material are capable to be as host for a Pd nanoparticles.

The presence of palladium in the catalyst was confirmed by ICP, which showed a value of about 0.14 mmol Pd per gram of catalyst.

Figures 3a, b and c present the field emission scanning electron microscopy (FE−SEM) images of nanosilica, nSTDP and Pdnp−nSTDP. The size and surface morphologies of the nSTDP and Pd$_{np}$−nSTDP are uniform, as shown in the images, the nSiO$_2$ particles are spherical and the average diameters are in the range of 50 to 70 nm.

The energy dispersive X−ray (EDX) results, collected from SEM analysis, proved the presence of S and Si elements in the nSTDP and also Pd element in the Pd$_{np}$−nSTDP (Figures 3d and e). Elemental mapping of Pd$_{np}$−nSTDP depicted in Figure 4, in which the uniform and homogenous dispersion of C, Si, O, S and Pd elements can be visualized.

Figure 5A shows the transmission electron microscopy (TEM) image of the Pd$_{np}$−nSTDP. The picture verifies that the particles are well dispersed and almost no agglomeration was observed. Also, the catalyst composed of spherical, nanosized Pd particles range from 2 to 5.5 nm (Figure 5B).

X-ray photoelectron spectroscopy (XPS) is a powerful tool to investigate the electron properties of the species formed on the surface, such as the electron environment, oxidation state, and the binding energy of the core electron of the metal. Figure 6 shows the XPS spectrum of catalyst. The calibration was performed with the C1s peak (E= 284.5 eV). As shown in this Figure, the peaks at 335.85 (3d5/2) and 340.98 eV (3d3/2), correspond to Pd with zero oxidation state.[62] The peaks corresponding to silicon, oxygen, carbon, sulfur and palladium are also clearly observed in XPS elemental survey of the catalyst (Figure 6).

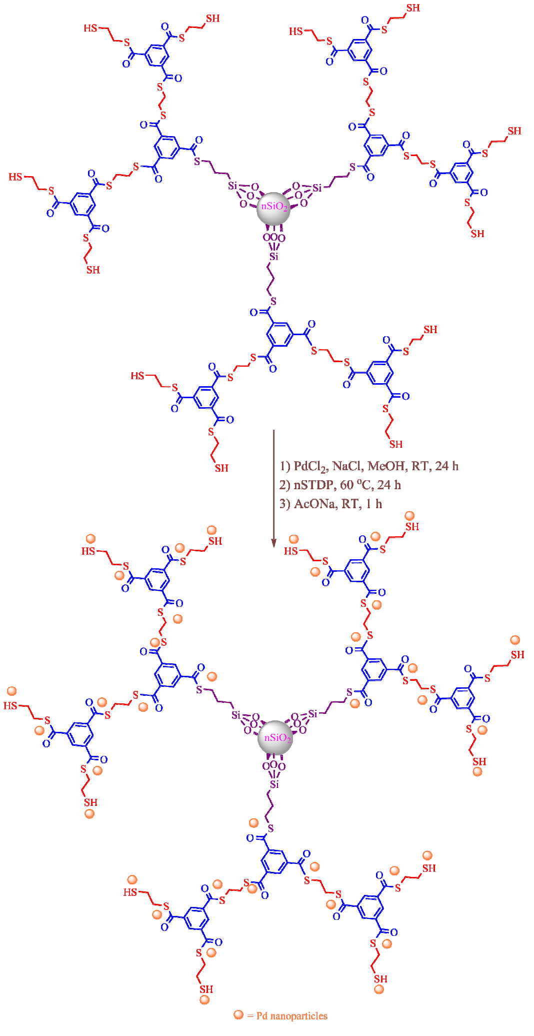

Scheme 3. Synthesis of the Pd$_{np}$−nSTDP catalyst

All these observations confirm that this new thiolated dendritic polymer is an appropriate host and ligand for palladium nanoparticles.

View Article Online
DOI: 10.1039/C6RA16704G

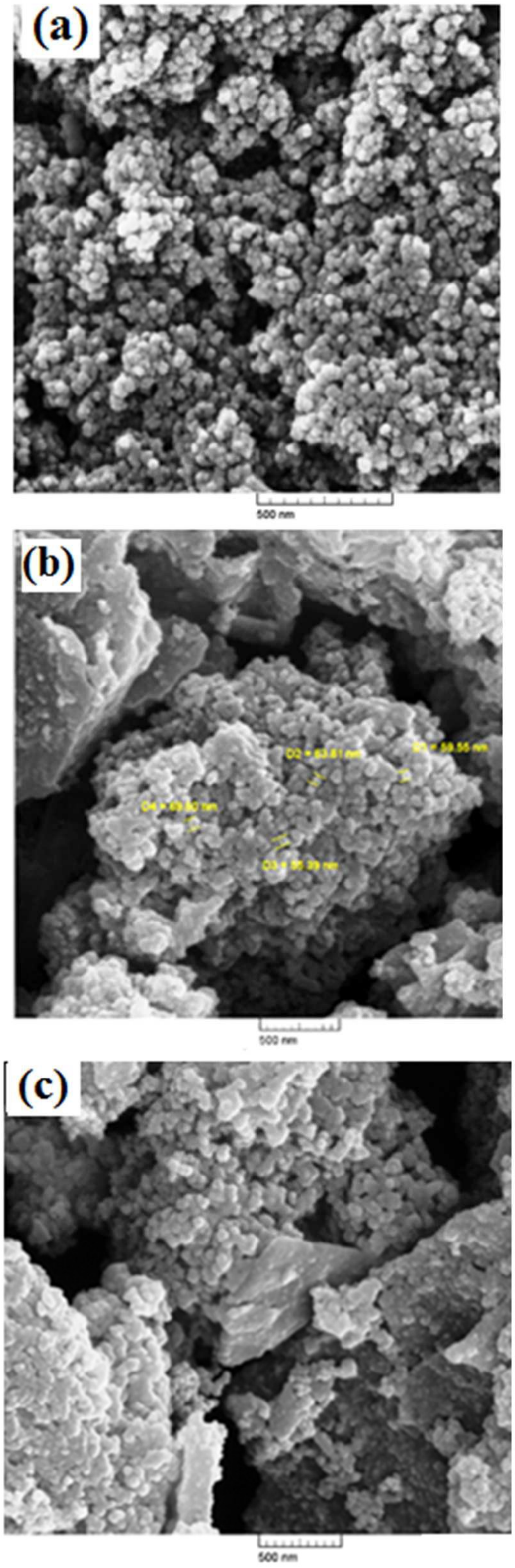

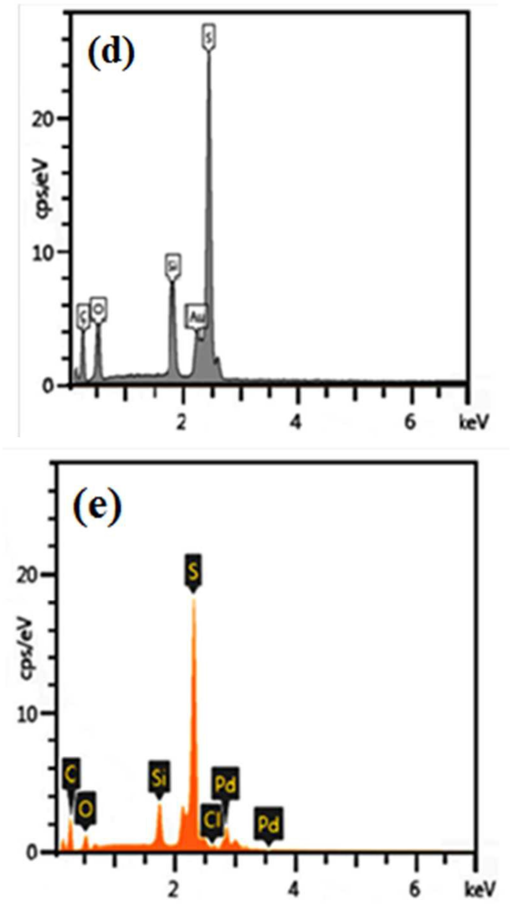

Fig. 3. FE–SEM images of: a) nanosilica, b) nSTDP and c) Pd_{np}–nSTDP. SEM–EDX spectra of: d) nSTDP and e) Pd_{np}–nSTDP.

Catalytic experiments

The catalytic activity of the prepared catalyst was investigated in the Suzuki-Miyaura and Heck C-C coupling reactions.

Suzuki–Miyaura Coupling of Aryl Halides with Arylboronic Acids

The Suzuki–Miyaura cross−coupling reactions typically require careful optimization of base and solvent types, temperature, amount of catalyst and substrates molar ratios (Table 2). In this manner, the Suzuki–Miyaura cross−coupling of 4−iodoanisole with phenylboronic acid in the presence of Pd_{np}−nSTDP catalyst was selected as a model for optimization of reaction parameters such as the base and solvent types, temperature, amount of catalyst and substrates molar ratios (Table 2).

To optimize the solvent, different types of single and mixed solvents were employed. The mixture of DMF/H_2O (1:2) was proved to be the optimum reaction medium (Table 2, entries 1-7). Several organic and inorganic bases were screened (i.e., NEt_3, DBU, Na_2CO_3, K_3PO_4, NaOH, piperidine and K_2CO_3), of which K_2CO_3 gave the best yield (Table 2, entries 8-14). A 1:1.1:1.5 ratio of 4−iodoanisole to phenylboronic acid and base was optimal for product formation. The catalytic loading could

View Article Online
DOI: 10.1039/C6RA16704G

be lowered to 0.07 mol% Pd (5 mg) with shorter reaction times and up to 98% yield.

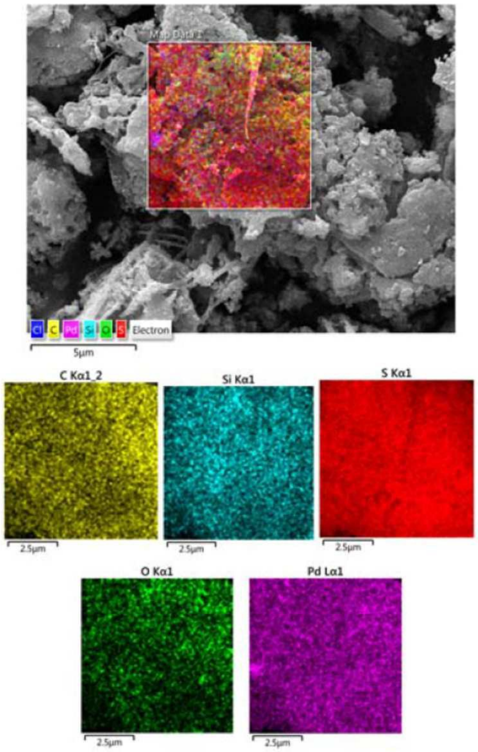

Fig. 4. Elemental mapping (S, Si, C, O and Pd) of Pd$_{np}$–nSTDP.

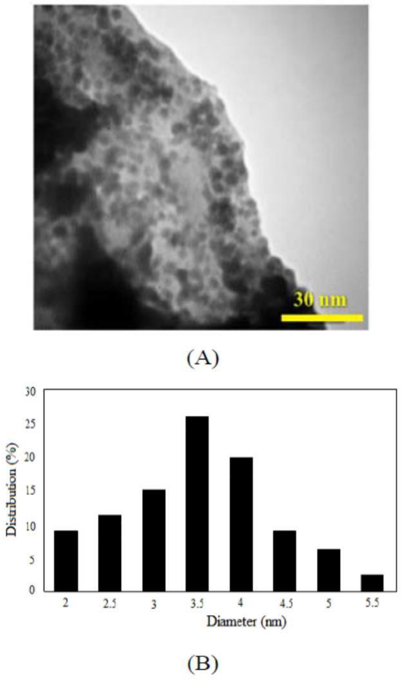

(A)

(B)

Fig. 5. (A) TEM image for Pd$_{np}$–nSTDP and (B) Particle size distribution results for Pd$_{np}$–nSTDP catalyst.

However, decreasing the catalyst loading, led to longer reaction time and lower yield (Table 2, entry 17).

The effect of reaction temperature was also investigated and the 60 °C was suitable for evaluation of the scope of Suzuki–Miyaura cross−coupling reaction.

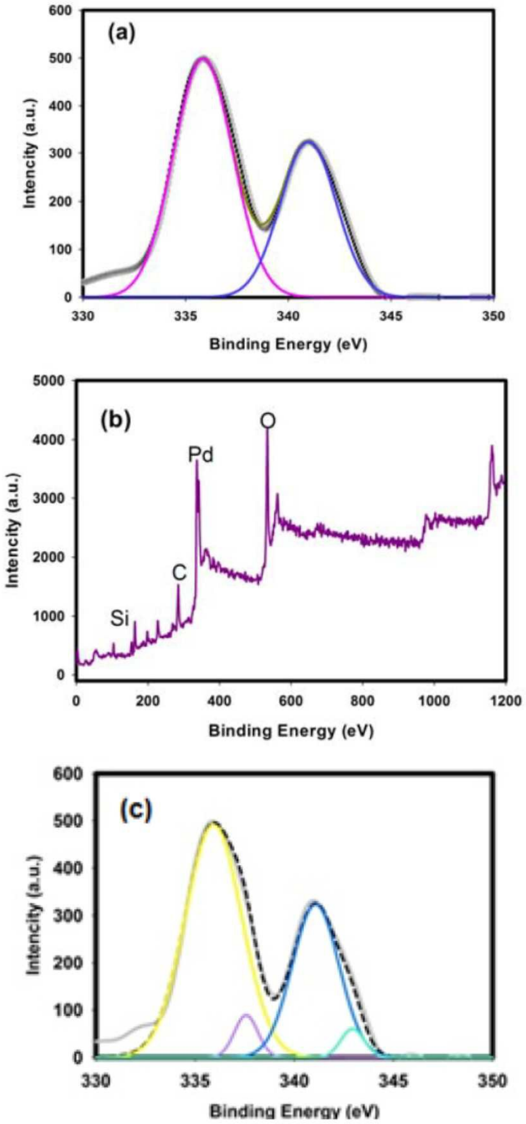

Fig. 6. The XPS spectra of catalyst: (a) showing Pd 3d$_{5/2}$ and Pd 3d$_{3/2}$ binding energies, (b) the elemental survey scan, (c) Reused Pd$_{np}$–nSTDP

To determine the substrate scope for the Suzuki–Miyaura cross−coupling reaction, different aryl halides were employed in the reaction (Table 3). In this case, different substituted aryl chloride, bromide and iodides were reacted with phenylboronic acid and 4−methoxyphenylboronic acid in the presence of 0.07 mol% (5 mg) of Pd$_{np}$−nSTDP as catalyst, K_2CO_3 as base and DMF/H_2O (2:1) as solvent. The experimental data showed that reactions proceeded extremely well and the electronic properties of the substituents and functional groups on the aromatic rings had almost negligible effect on the results.

DOI: 10.1039/C6RA16704G

Further investigation also revealed that aryl iodides were more reactive than aryl bromides and aryl chlorides in these catalytic reactions. Although, aryl chlorides have less reactivity than aryl iodides and aryl bromides, but they are economically more available. Due to less reactivity, the coupling reactions with aryl chlorides have been performed at 90 °C (Table 3, entries 14−18).[63,64]

Heck Reaction of Aryl Halides with Styrenes

The high catalytic activity of this catalyst in the Suzuki–Miyaura cross−coupling reaction prompted us to investigate the catalytic capability of our new designed dendritic polymer-supported palladium particles in the Heck reaction.

For identifying the exact optimized conditions for the coupling reaction detailed in Table 4, the reaction of 4−bromoacetophenone and styrene was selected as a model reactin using Pd_{np}−nSTDP as catalyst under thermal conditions. The optimized conditions were gained applying 4−bromoacetophenone (1 mmol), styrene (1.1 mmol), K_2CO_3 (1.5 mmol) and Pd_{np}−nSTDP 0.14 mol% Pd (10 mg) in DMF/H_2O (1:2) at 95 °C.

The substrate scope of the coupling reaction was investigated using various structurally different aryl halides (Table 5). As it is mentioned in Table 5, the yield were decreased from aryl halides to bromides and chlorides. While the nature of substituents of R^1 and R^2 has almost no specific effect on the reaction.

Catalyst Recycling and Reuse

From industrial and economic points of view, the catalyst recycling is the most important issue for a heterogeneous catalyst. Therefore, the reusability of the $\mathrm{Pd}_{\mathrm{np}}$−nSTDP catalyst was investigated in the Suzuki–Miyaura cross−coupling reaction of 4−iodoanisole with phenylboronic acid and Heck reaction of 4−bromoacetophenone with styrene under the optimized conditions. After completion of each catalytic cycle, the catalyst was separated by simple filtration and reused. The results showed that the catalyst could be reused five consecutive times without significant loss of its catalytic activity in both reactions (Table 6). The analysis of palladium leaching from $\mathrm{Pd}_{\mathrm{np}}$−nSTDP catalyst by ICP indicated that only a negligible amount of palladium has been leached in the first two runs in the Suzuki-Miyaura reaction and in the first three runs in the Heck reaction. The hot filtration test was also carried out in both reactions. In this manner, the hot reaction mixtures were centrifuged at about 45% conversion to remove the solid particles. The filtrates continue to catalyze the reactions. Compared to the unfiltered reaction (after 15 min for Suzuki-Miyaura and 12 h for Heck reaction), no further progress was observed.

The XPS studies on the recycled catalyst prove the presence of Pd nanoparticles in the texture. However the spectra shows the existence of small amounts of Pd(II) which was not observed in freshly prepared catalyst. This indicates that some Pd nanoparticles were oxidized to Pd(II) (Fig. 6c).[65]

The results of the present study were compared with some results reported in the Suzuki-Miyaura cross-coupling and Heck reaction catalyzed by different Pd containing catalysts. As can be seen, this catalytic system is more efficient than the others in the Suzuki-Miyaura cross-coupling reaction by comparison of their TOFs (Table 7). Also, in the case Heck reaction, the TOFs show that this catalytic system is one of the best catalytic systems (Table 8).

Table 2. Optimization of the Suzuki–Miyaura cross−coupling of 4−iodoanisole (IA) with phenylboronic acid (PBA) catalyzed by Pd_{np}−nSTDP.

Entry	Base	Ba:PBA:Base (mmol)	Catalyst (mol% Pd)	Solvent[a]	T (°C)	Time (min)	Yield (%)[b]
1	K_2CO_3	1:1.1:1.5	0.07	Toluene	60	45	50
2	K_2CO_3	1:1.1:1.5	0.07	EtOH	60	70	63
3	K_2CO_3	1:1.1:1.5	0.07	EtOH/H_2O (1:1)	60	50	75
4	K_2CO_3	1:1.1:1.5	0.07	DMF	60	80	65
5	K_2CO_3	1:1.1:1.5	0.07	H_2O	60	80	59
6	K_2CO_3	1:1.1:1.5	0.07	DMF/H_2O (1:1)	60	25	85
7	K_2CO_3	1:1.1:1.5	0.07	DMF/H_2O (2:1)	60	10	98
8	NEt_3	1:1.1:1.5	0.07	DMF/H_2O (2:1)	60	50	54
9	DBU[c]	1:1.1:1.5	0.07	DMF/H_2O (2:1)	60	50	46
10	Na_2CO_3	1:1.1:1.5	0.07	DMF/H_2O (2:1)	60	30	50
11	K_3PO_4	1:1.1:1.5	0.07	DMF/H_2O (2:1)	60	45	50
12	NaOH	1:1.1:1.5	0.07	DMF/H_2O (2:1)	60	50	54
13	Piperidine	1:1.1:1.5	0.07	DMF/H_2O (2:1)	60	50	30
14	K_2CO_3	1:1:1	0.07	DMF/H_2O (2:1)	60	25	80
15	K_2CO_3	1:1:1.2	0.07	DMF/H_2O (2:1)	60	25	85
16	K_2CO_3	1:1:1.5	0.07	DMF/H_2O (2:1)	60	30	85
17	K_2CO_3	1:1.1:1.5	0.04	DMF/H_2O (2:1)	60	20	90
18	K_2CO_3	1:1.1:1.5	0.014	DMF/H_2O (2:1)	60	10	98
19	K_2CO_3	1:1.1:1.5	0.07	DMF/H_2O (2:1)	25	30	65
20	K_2CO_3	1:1.1:1.5	0.07	DMF/H_2O (2:1)	40	25	80

a) Reaction was performed using 3 ml of solvent.

b) GC yield

c) 1,8-Diazabicyclo [5.4.0] undec-7-ene

View Article Online
DOI: 10.1039/C6RA16704G

Table 3. Suzuki–Miyaura cross−coupling of aryl halides with arylboronic acids catalyzed by Pd_{np}−nSTDP.[a]

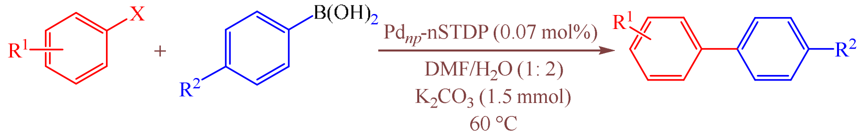

Entry	R^1	R^2	X	Time (min)	Yield (%)[b]	TOF (h^{-1})
1	H	H	I	10	95	8143
2	H	4−MeO	I	10	98	8400
3	4−Ac	H	I	15	92	5257
4	4−Ac	4−MeO	I	13	95	6263
5	4−Me	H	I	10	95	8143
6	H	4−MeO	Br	30	94	2685
7	H	H	Br	25	95	3257
8	4−MeO	4−MeO	Br	30	93	2657
9	4−MeO	H	Br	28	96	2939
10	4−Ac	4−MeO	Br	32	91	2437
11	4−Ac	H	Br	30	93	2657
12	4−CHO	4−MeO	Br	35	91	2228
13	4−CHO	H	Br	32	93	2491
14	H[c]	4−MeO	Cl	40	81	1735
15	H[c]	H	Cl	38	82	1849
16	4−Ac[c]	4−MeO	Cl	65	85	1120
17	4−Ac[c]	H	Cl	55	87	1355
18	4−CHO[c]	H	Cl	65	90	1186

a) Reaction conditions: Aryl halide (1 mmol), phenylboronic acid (1.1 mmol), K_2CO_3 (1.5 mmol), Pd_{np}−nSTDP (0.005 g, 0.07 mol% Pd), H_2O/DMF (1 mL/2 mL) at 60 °C.

b) GC yield

c) The reaction was performed at 90 °C

Table 4. Optimization of the Heck reaction of 4−bromoacetophenone (BA) with styrene (Sty) catalyzed by Pd_{np}−nSTDP.[a]

Entry	Base	BA:Sty:Base (mmol)	Catalyst (mol% Pd)	Solvent[a]	T (°C)	Time (h)	Yield (%)[b]
1	K_2CO_3	1:1.1:1.5	0.14	Toluene	95	22	55
2	K_2CO_3	1:1.1:1.5	0.14	EtOH	95	25	50
3	K_2CO_3	1:1.1:1.5	0.14	H_2O	95	15	65
4	K_2CO_3	1:1.1:1.5	0.14	EtOH/H_2O (1:1)	95	18	60
5	K_2CO_3	1:1.1:1.5	0.14	DMF	95	14	65
6	K_2CO_3	1:1.1:1.5	0.14	DMF/H_2O (1:1)	95	12	68
7	K_2CO_3	1:1.1:1.5	0.14	DMF/H_2O (2:1)	95	8	94
8	NEt_3	1:1.1:1.5	0.14	DMF/H_2O (2:1)	95	20	50
9	DBU	1:1.1:1.5	0.14	DMF/H_2O (2:1)	95	22	55
10	Na_2CO_3	1:1.1:1.5	0.14	DMF/H_2O (2:1)	95	14	60
11	K_3PO_4	1:1.1:1.5	0.14	DMF/H_2O (2:1)	95	18	60
12	NaOH	1:1.1:1.5	0.14	DMF/H_2O (2:1)	95	15	55
13	K_2CO_3	1:1:1	0.14	DMF/H_2O (2:1)	95	18	45
14	K_2CO_3	1:1.1:1.2	0.14	DMF/H_2O (2:1)	95	14	70
15	K_2CO_3	1:1.1:1.5	0.07	DMF/H_2O (2:1)	95	10	75
16	K_2CO_3	1:1.1:1.5	0.21	DMF/H_2O (2:1)	95	8	94
17	K_2CO_3	1:1.1:1.5	0.14	DMF/H_2O (2:1)	80	12	85
18	K_2CO_3	1:1.1:1.5	0.14	DMF/H_2O (2:1)	110	8	94

a) The reaction was performed using 3 ml of solvent.

b) GC yield

View Article Online
DOI: 10.1039/C6RA16704G

Table 5. Heck reaction of aryl halides with styrenes catalyzed by Pd$_{np}$−nSTDP.[a]

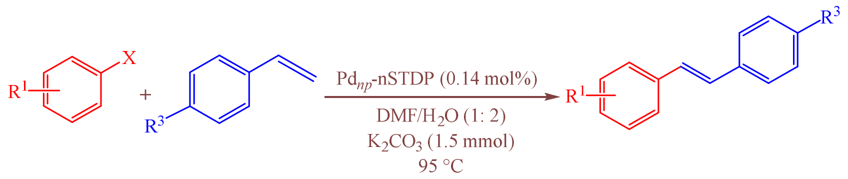

Entry	R^1	R^2	X	Time (h)	Yield (%)[b]	TOF (h^{-1})
1	H	H	I	7.5	96	91.43
2	H	4−Me	I	8	94	83.93
3	4−Ac	H	I	8	95	84.82
4	4−Ac	4−Me	I	8	94	83.93
5	4−Me	H	I	8	95	84.82
6	H	H	Br	11	93	60.39
7	H	4−Me	Br	10	91	65
8	4−F	H	Br	11	92	59.74
9	4−Ac	H	Br	12	94	55.95
10	4−Ac	4−Me	Br	11	93	60.39
11	4−CHO	H	Br	12	91	54.16
12	4−MeO	4−Me	Br	12	92	54.76
13	H	H	Cl	16	91	40.62
14	4−Ac	4−Me	Cl	16	89	39.73
15	4−Ac	H	Cl	15	88	41.90
16	4−CHO	H	Cl	16	88	39.28

a) Reaction conditions: Aryl halide (1 mmol), styrenes (1.1 mmol), K_2CO_3 (1.5 mmol), Pd$_{np}$−nSTDP (0.01 g, 0.14 mol% Pd), H_2O/DMF (1 mL/2 mL) at 95 °C.

b) GC yield

Table 6. Recycling of the Pd$_{np}$−nSTDP catalyst in the Suzuki-Miyaura cross−coupling of 4−bromoacetophenone with phenylboronic acid in 15 min[a] and Heck reaction of 4−bromoacetophenone with styrene after 12 h.[b]

Run	Yield (%)[c]		Pd leached (%)[d]	
	Suzuki-Miyaura	Heck reaction	Suzuki-Miyaura	Heck reaction
1	92	94	2	4
2	90	90	1	2
3	88	86	0	1.5
4	88	86	0	0
5	88	86	0	0

a) Reaction conditions: 4−bromoacetophenone (1 mmol), phenylboronic acid (1.1 mmol), K_2CO_3 (1.5 mmol), Pd$_{np}$−nSTDP (0.005 g, 0.07 mol% Pd), H_2O/DMF (1 mL/2 mL) at 60 °C.

b) Reaction conditions: 4−bromoacetophenone (1 mmol), styrene (1.1 mmol), K_2CO_3 (1.5 mmol), Pd$_{np}$−nSTDP (0.01 g, 0.14 mol% Pd), H_2O/DMF (1 mL/2 mL) at 95 °C.

c) GC yield.

d) Determined by ICP analysis

Conclusion

This paper describes the synthesis and characterization of a new thiol based dendritic material as a host for carrying of palladium nanoparticles. The new synthesized nanosilica thiolated dendritic polymer-supported Pd particles has proven to be highly effective heterogeneous catalyst for carbon−carbon couplings in both Suzuki-Miyaura and Heck reactions. Although palladium as a precious metal is quite expensive, we have shown that they can be easily recovered and reused for several times, without any significant loss of its catalytic activity. Therefor it would be possible to use them in further real−world applications.

Table 7. Comparison of the results obtained in the Suzuki-Miyaura coupling reaction of bromobenzene with phenylboronic acid catalyzed by Pd$_{np}$−nSTDP with those obtained by some recently reported catalysts.

Catalyst	Reaction conditions	TOF (h^{-1})	Ref
Pd(0)/UiO-66-NH$_2$	DMF/H_2O, K_2CO_3, 60 °C, 30 min	697.7	37
Pd(PyBNHC)@nSiO$_2$	DMF/H_2O, K_2CO_3, 65 °C, 100 min	438	67
Pd(0)/MCoS-1	H_2O, K_2CO_3, 70 °C, 300 min	98	66
PdTN	THF/H_2O,NaOH, 63 °C, 150 min	80	48
Pd Schiff base complex	DMF/H_2O, K_2CO_3, 100 °C, 1440 min	16.6	64
Pd−nSTDP	DMF/H_2O, K_2CO_3, RT, 360 min	2666	11
Pd*np*−nSTDP	DMF/H_2O, K_2CO_3, 60 °C, 25 min	3257	This work

View Article Online
DOI: 10.1039/C6RA16704G

Table 8. Comparison of the results obtained in the Heck reaction of 4-bromobenzenel with styrene catalyzed by Pd$_{np}$−nSTDP with those obtained by some reported catalysts.

Catalyst	Reaction conditions	TOF (h^{-1})	Ref
Pd(OAc)$_2$/(LHX)	DMF/H$_2$O, K$_2$CO$_3$, 80 °C, 4 h	15.5	68
Palladacycle	[n-Bu$_4$N]Br, Na(OAc), 120 °C, 16 h	62.5	69
Pd/USY	DMF, NaOAc, H$_2$, 140 °C, 20 h	48	70
Pd(OAc)$_2$/NHC	DMF/H$_2$O, K$_2$CO$_3$, 80 °C, 2 h	24	71
Pd@PANI	DMF, N$_2$, EtN(i-Pr)$_2$, 120 °C, 48 h	14.5	72
Pd−nSTDP	DMF/H$_2$O, K$_2$CO$_3$, 85 °C, 14 h	642	11
PEPSI-Pd NHC	DMF, K$_2$CO$_3$, TBAB, 140 °C, 2 h	100	73
Pd$_{np}$−nSTDP	DMF/H$_2$O, K$_2$CO$_3$, 95 °C, 11 h	60.4	This work

Acknowledgement

Partial support of this work by the Research Council of the University of Isfahan is acknowledged.

References

1 D. A. Tomalia and J. M. J. Frechet, Discovery of dendrimers and dendritic polymers: a brief historical perspective. *J. Polym. Sci. A: Polym. Chem*. 2002, **9**, 2719–2728.

2 F. Vögtle, G. Richardt and N. Werner, Dendrimer Chemistry Concepts, Synthesis, Properties, Applications, Wiley−VCH, Weinheim, 2009.

3 A. W. Bosman, H. M. Janssen and E. W. Meijer, About Dendrimers: Structure, Physical Properties, and Applications. *Chem. Rev*. 1999, **99**, 1665–1688.

4 D. Astruc, E. Boisselier and C. Ornelas, Dendrimers Designed for Functions: From Physical, Photophysical, and Supramolecular Properties to Applications in Sensing, Catalysis, Molecular Electronics, Photonics, and Nanomedicine. *Chem. Rev*. 2010, **110**, 1857–1959.

5 G. R. Newkome and C. N. Moorefield, Suprasupermolecules with Novel Properties: Metallodendrimers. *Chem. Rev.* 1999, **99**, 1689–1746.

6 G. M. Dykes, Dendrimers: a review of their appeal and applications. *J. Chem. Technol. Biotechnol*. 2001, **76**, 903–918.

7 B. Klajnert and M. Bryszewska, Dendrimers: properties and applications. *Acta Biochim. Pol*. 2001, **48**, 199−208.

8 S. M. Grayson and J. M. J. Frechet, Convergent dendrons and dendrimers: From synthesis to applications. *Chem. Rev.* 2001, **101**, 3819−3867.

9 V. S. Myers, M. G. Weir, E. V. Carino, D. F. Yancey, S. Pande and R. M. Crooks, Dendrimer-encapsulated nanoparticles: New synthetic and characterization methods and catalytic applications. *Chem. Sci.* 2011, **2**, 1632−1646.

10 M. A. Herrero, J. Guerra, V. S. Myers, M. V. Gomez, R. M. Crooks and M. Prato, Gold Dendrimer Encapsulated Nanoparticles as Labeling Agents for Multiwalled Carbon Nanotubes. *ACS Nano*. 2010, **4,** 905−912.

11 A. Landarani Isfahani, I. Mohammadpoor−Baltork, V. Mirkhani, A. R. Khosropour, M. Moghadam, S. Tangestaninejad and R. Kia, Palladium Nanoparticles Immobilized on Nano-Silica Triazine Dendritic Polymer (Pd$_{np}$-nSTDP): An Efficient and Reusable Catalyst for Suzuki–Miyaura Cross-Coupling and Heck Reactions. *Adv. Synth. Catal*. 2013, **355**, 957–972.

12 J. H. Noh, R. Patala and R. Meijboom, Catalytic evaluation of dendrimer and reverse microemulsion template Pd and Pt nanoparticles for the selective oxidation of styrene using TBHP. *Appl. Catal. A*: *Gen*. 2016, **514**, 253–266.

13 J. H and Noh, R. Meijboom, Dendrimer-templated Pd nanoparticles an Pd nanoparticles synthesized by reverse microemulsions as efficient nanocatalyst for the Heck reaction: A comparative study. *J. Colloid Interface Sci*. 2014, **415**, 57–69.

14 M. Nasr−Esfehani, I. Mohammadpoor−Baltork, A. R. Khosropour, M. Moghadam, V. Mirkhani and S. Tangestaninejad, Synthesis and characterization of Cu(II) containing nanosilica triazine dendrimer: A recyclable nanocomposite material for the synthesis of benzimidazoles, benzothiazoles, *bis*-benzimidazoles and *bis*-benzothiazoles. *J. Mol. Catal. A: Chem.* 2013, **379**, 243−259.

15 Z. V. Feng, J. L. Lyon, J. S. Croley, R. M. Crooks, D. A. Vanden Bout and K. J. Stevenson, Synthesis and catalytic evaluation of dendrimer-encapsulated Cu nanoparticles. *J. Chem. Educ*. 2009, **86**, 368–372.

16 N. C. Beck Tan, L. Balogh, S. F. Trevino, D. A. Tomalia and J. S. Lin, A small angle scattering study of dendrimer–copper sulfide nanocomposites. *Polymer* 1999, **40**, 2537−2545.

17 P. Kracke, T. Haas, H. Saltsburg and M. Flytzani-Stephanopoulos, CO Oxidation on Unsupported Dendrimer-Encapsulated Gold Nanoparticles. *J. Phys. Chem. C*, 2010, **114**, 16401–16407.

18 T. Mandal, C. Dasgupta and P. K. Maiti, Engineering Gold Nanoparticle Interaction by PAMAM Dendrimer. *J. Phys. Chem. C,* 2013, **117**, 13627–13636.

19 M. Stemmler, F. D. Stefani, S. Bernhardt, R. E. Bauer, M. Kreiter, K. Müllen and W. Knoll, One-Pot Preparation of Dendrimer−Gold Nanoparticle Hybrids in a Dipolar Aprotic Solvent. *Langmuir* 2009, **25**, 12425–12428.

20 X. Yuan, S. Wen, M. Shen and X. Shi, Dendrimer-stabilized silver nanoparticles enable efficient colorimetric sensing of mercury ions in aqueous solution; *Anal. Methods*, 2013, **5**, 5486–5492.

21 M. Zhao and R. M.Crooks, Dendrimer-Encapsulated Pt Nanoparticles: Synthesis, Characterization, and Applications to Catalysis. *Adv. Mater*. 1999, **11***,* 217−220.

22 K. Esumi, A. Suzuki, A. Yamahira and K. Torigoe, Role of Poly(amidoamine) Dendrimers for Preparing Nanoparticles of Gold, Platinum, and Silver. *Langmuir* 2000, **16**, 2604−2608.

23 N. C. Antonels and R. Meijboom, Preparation of well-defined dendrimer encapsulated ruthenium nanoparticles and their application as catalyst and enhancement of activity when utilised as SCILL catalysts in the hydrogenation of citral. *Catal. Commun.* 2014, **57**, 148–152.

24 N. C. Antonels and R. Meijboom, Preparation of well-defined dendrimer encapsulated ruthenium nanoparticles and their evaluation in the reduction of 4-nitrophenol according to the Langmuir-Hinshelwood approach. *Langmuir* 2013, **29**, 13433–13442.

25 R. M. Crooks, M. Zhao, L. Sun, V. Chechik and L. Yeung, Dendrimer-Encapsulated Metal Nanoparticles: Synthesis, Characterization, and Applications to Catalysis, *Acc. Chem. Res*. 2001, **34**, 181-190.

View Article Online
DOI: 10.1039/C6RA16704G

26 T. Liu, L. Xie, Y. Li, X. Li, S. Pang and T. Zhang, Hydrogen/deuterium storage properties of Pd nanoparticles. *J. Power Sources*, 2013, **237**, 74–79.

27 D. Gupta, D. Dutta, M. Kumar, P. B. Barman, C. K. Sarkar, S. Basu and S. K. Hazra, A low temperature hydrogen sensor based on palladium nanoparticles. *Sensors Actuat. B: Chem.* 2014, **196**, 215–222.

28 J. Yu, R. Y. F. Liu, B. Poon, S. Nazarenko, T. Koloski, T. Vargo, A. Hiltner and E. Baer, Polymers with palladium nanoparticles as active membrane materials. *J. Appl. Polym. Sci.* 2004, **92**, 749−756.

29 I. Feliciano−Ramos, B. Casañas−Montes, M. M. García−Maldonado, C. L. Menéndez, A. R. Mayol, L. M. Díaz−Vázquez and C. R. Cabrera, Assembly of a Cost-Effective Anode Using Palladium Nanoparticles for Alkaline Fuel Cell Applications. *J. Chem. Edu.* 2015, **92**, 360–363.

30 J. Huang, T. Jiang, B. Han, H. Gao, Y. Chang, G. Zhao and W. Wu, Hydrogenation of olefins using ligand-stabilized palladium nanoparticles in an ionic liquid. *Chem. Commun.* 2003, **14**, 1654−1655.

31 X. Gu, Z. H. Lu, H. L. Jiang, T. Akita and Q. Xu, Synergistic catalysis of metal-organic framework-immobilized Au-Pd nanoparticles in dehydrogenation of formic acid for chemical hydrogen storage. *J. Am. Chem. Soc*. 2011, **133***,* 11822–11825.

32 M. Moreno−Mañas and R. Pleixats, Formation of Carbon−Carbon Bonds under Catalysis by Transition-Metal Nanoparticles. *Acc. Chem. Res*. 2003, **36**, 638–643.

33 M. K. Chung and M. Schlaf, A Catalytic Synthesis of Thiosilanes and Silthianes: Palladium Nanoparticle-Mediated Cross-Coupling of Silanes with Thio Phenyl and Thio Vinyl Ethers through Selective Carbon−Sulfur Bond Activation. *J. Am. Chem. Soc*. 2004, **126***,* 7386–7392.

34 V. Kogan, Z. Aizenshtat, R. Popovitz−Biro and R. Neumann, Carbon-carbon and carbon-nitrogen coupling reactions catalyzed by palladium nanoparticles derived from a palladium substituted Keggin-type polyoxometalate. *Org. Lett*. 2002, **4**, 3529–3532.

35 B. J. Gallon, R. W. Kojima, R. B. Kaner and P. L. Diaconescu, Palladium Nanoparticles Supported on Polyaniline Nanofibers as Semi-Heterogeneous Catalysts in Water, *Angew. Chem. Int. Ed.* 2007, **46***,* 7251-7254.

36 S. Harish, J. Mathiyarasu, K. L. N. Phani and V. Yegnaraman, Synthesis of Conducting Polymer Supported Pd Nanoparticles in Aqueous Medium and Catalytic Activity Towards 4-Nitrophenol Reduction. *Catal. Lett*. 2009, **128**, 197−202.

37 E. Groppo, G. Agostini, E. Borfecchia, L. Weit, F. Giannici, G. Portale, A. Longo and C. Lamberti, Formation and Growth of Pd Nanoparticles Inside a Highly Cross-Linked Polystyrene Support: Role of the Reducing Agent. *J. Phys. Chem. C,* 2014, **118**, 8406−8415.

38 J. Mondal, A. Modak and A. Bhaumik, One-pot efficient Heck coupling in water catalyzed by palladium nanoparticles tethered into mesoporous organic polymer, *J. Mol, Catal A: Chem*, 2011, **350**, 40-48.

39 R. Kardanpour, S. Tangestaninejad, V. Mirkhani, M. Moghadam, I. Mohammadpoor−Baltork, A. R. Khosropour and F. Zadehahmadi, Highly dispersed palladium nanoparticles supported on amino functionalized metal-organic frameworks as an efficient and reusable catalyst for Suzuki cross-coupling reaction. *J. Organomet. Chem.* 2014, **761**, 127−133.

40 P. Lan, D. Berta, J. A. Porco, M. S. South and J. J. Parlow, Polymer-Assisted Solution-Phase (PASP) Suzuki Couplings Employing an Anthracene-Tagged Palladium Catalyst. *J. Org. Chem*. 2003, **68***,* 9678–9686.

41 Z. Pahlevanneshan, M. Moghadam, V. Mirkhani, S. Tangestaninejad, I. Mohammadpoor−Baltork and A. R. Khosropour, Immobilization of palladium(II)-containing *bis*(imidazolium) ligand on ion-exchange resins: efficient and reusable catalysts for C–C coupling reactions. *Appl. Organomet. Chem*. 2015, **29**, 346–352.

42 D. J. Gavia and Y. S. Shon, Controlling Surface Ligand Density and Core Size of Alkanethiolate-Capped Pd Nanoparticles and Their Effects on Catalysis. *Langmuir*, 2012, **28**, 14502-14508.

43 C. M. A. Parlett, D. W. Bruce, N. S. Hondow, A. F. Lee and K. Wilson, Support-Enhanced Selective Aerobic Alcohol Oxidation over Pd/Mesoporous Silica. *ACS Catal.*, 2011, **1**, 636−640.

44 M. Ruta, N. Semagina and L. Kiwi−Minsker, Monodispersed Pd Nanoparticles for Acetylene Selective Hydrogenation: Particle Size and Support Effects. *J. Phys. Chem. C* 2008, *112,* 13635−13641.

45 J. C. Garcia-Martinez, R. Lezutekong and R. M. Crooks, Dendrimer-Encapsulated Pd Nanoparticles as Aqueous, Room Temperature Catalysts for the stille Reaction. *J. Am. Chem. Soc*. 2005, **127**, 5097−5103.

46 E. V. Carino, M. R. Knecht and R. M. Crooks, Quantitative Analysis of the Stability of Pd Dendrimer-Encapsulated Nanoparticles. *Langmuir* 2009, **25**, 10279−10284.

47 X. Zhang, J. Zhu, C. S. Tiwary, Z. Ma, H. Huang, J. Zhang, Z. Lu, W. Huang and Y. Wu. Palladium Nanoparticles Supported on Nitrogen and Sulfur Dual-Doped Graphene as Highly Active Electrocatalysts for Formic Acid and Methanol Oxidation. *ACS Appl. Mater. Interfaces,* 2016, **8**, 10858−10865.

48 F. Lu, J. Ruiz and D. Astruc, Palladium–dodecanethiolate nanoparticles as stable and recyclable catalysts for the Suzuki–Miyaura reaction of aryl halides under ambient conditions. *Tetrahedron Lett*. 2004, **45**, 9443−9445.

49 J. Alvarez, J. Liu, E. Román and A. E. Kaifer, Water-Soluble Platinum and Palladium Nanoparticles Modified with Thiolated β-Cyclodextrin, *Chem. Commun.* 2000, **13**, 1151-1152.

50 Xiong, Y.; Xia, Y. Shape-Controlled Synthesis of Metal Nanostructures: The Case of Palladium. *Adv. Mater*. 2007, **19**, 3385−3391.

51 B. Lim, M. Jiang, J. Tao, P. H. C. Camargo, Y. Zhu and Y. Xia, Shape-Controlled Synthesis of Pd Nanocrystals in Aqueous Solutions. *Adv. Funct. Mater*. 2009, **19***,* 189−200.

52 A. Daneshvar, M. Moghadam, S. Tangestaninejad, V. Mirkhani, I. Mohammadpoor-Baltork, A. Khalili, Ruthenium Hydride Complex Supported on Gold Nanoparticle Cored Triazine Dendrimers for C−C Coupling Reactions. *Organometallics* 2016, **35**, 1747−1755.

53 B. Asadi, I. Mohammadpoor-Baltork, S. Tangestaninejad, M. Moghadam, V. Mirkhani, A. Landarani-Isfahani, Synthesis and characterization of Bi(III) immobilized on triazine dendrimer-stabilized magnetic nanoparticles: a reusable catalyst for synthesis of aminonaphthoquinones and bis-aminonaphthoquinones. *New J. Chem.* 2016, DOI:10.1039/C5NJ03050A

View Article Online
DOI: 10.1039/C6RA16704G

54 A. Landarani Isfahani, I. Mohammadpoor-Baltork, V. Mirkhani, A. R. Khosropour, M. Moghadam, S. Tangestaninejad, Pd Nanoparticles Immobilized on Nanosilica Triazine Dendritic Polymer: A Reusable Catalyst for the Synthesis of Mono-, Di-, and Trialkynylaromatics by Sonogashira Cross-Coupling in Water. *Eur. J. Org. Chem*. 2014, **2014***,* 5603–5609.

55 A. Landarani Isfahani, I. Mohammadpoor-Baltork, V. Mirkhani, M. Moghadam, A. R. Khosropour, S. Tangestaninejad, M. Nasr-Esfahani, H. Amiri Rudbari, Palladium Nanoparticles Immobilized on Nanosilica Triazine Dendritic Polymer (Pd_{np}-nSTDP) as Catalyst in the Synthesis of Mono-, Di-, and Trisulfides through C–S Cross-Coupling Reactions. *Synlett,* 2014, **25**, 645−652.

56 I. Mohammadpoor-Baltork, M. Moghadam, M. Nasr-Esfahani, A. R. Khosropour, S. Tangestaninejad, V. Mirkhani, A. Agabekov, H. Amiri Rudbari, Copper immobilized on nano-silica triazine dendrimer (Cu(II)-TD@nSiO_2) catalyzed synthesis of symmetrical and unsymmetrical 1,3-diynes under aerobic conditions and ambient temperature. *RSC Adv*. 2014, **4**, 14291−14296.

57 M. Nasr-Esfahani, I. Mohammadpoor-Baltork, A. R. Khosropour, M. Moghadam, V. Mirkhani, S. Tangestaninejad, H. Amiri Rudbari, Copper Immobilized on Nanosilica Triazine Dendrimer (Cu(II)-TD@nSiO_2)-Catalyzed Regioselective Synthesis of 1,4-Disubstituted 1,2,3-Triazoles and Bis- and Tris-Triazoles via a One-Pot Multicomponent Click Reaction. *J. Org. Chem.*, 2014, **79**, 1437–1443.

58 N. Tsubokawa, H. Ichioka, T. Satoh, S. Hayashi, K. Fujiki, Grafting of 'dendrimer-like' highly branched polymer onto ultrafine silica surface. *React. Funct. Polym*. 1998, **37**, 75–82.

59 V. I. Kovalenko, V. L. Furer, A. E. Vandyukov, R. R. Shagidullin, J. P. Majoral and A. M. Caminade, The vibrational spectra of elementoorganic starburst dendrimers. *J. Mol. Struct*. 2002, **604**, 45−56.

60 S. Yoo, J. D. Lunn, S. Gonzalez, J. A. Ristich, E. E. Simanek and F. Shantz, Engineering Nanospaces: OMS/Dendrimer Hybrids Processing Controllable Chemistry and Porosity. *Chem. Mater*. 2006, **18**, 2935-2942.

61 R. Bernini, S. Cacchi, G. Fabrizi, G. Forte, F. Petrucci, A. Prastaro, S. Niembro, A. Shafird and A. Vallribera, Perfluoro-tagged, phosphine-free palladium nanoparticles supported on silica gel: application to alkynylation of aryl halides, Suzuki–Miyaura cross-coupling, and Heck reactions under aerobic conditions. *Green Chem*. 2010, **12**, 150–158.

62 Moulder, J. F.; Stickle, W. F.; Sobol, P. E.; Bomben, K. D.; Handbook of X-ray Photoelectron Spectroscopy, Perkin-Elmer Corp., Eden Prairie, M. N., 1992, p. 118.

63 C. L. Deng, S. M. Guo, Y. X. Xie and J. H. Li, Mild and Ligand-Free Palladium-Catalyzed Cross-Couplings between Aryl Halides and Arylboronic Acids for the Synthesis of Biaryls and Heterocycle-Containing Biaryls. *Eur. J. Org. Chem*. 2007, 1457–1462.

64 I. D. Kostas, B. R. Steele, A. Terzis, S. V. Amosova, A. V. Martynov and N. A. Makhaeva, New Palladium Complexes with S- or Se-Containing Schiff-Base Ligands as Efficient Catalysts for the Suzuki–Miyaura Cross-Coupling Reaction of Aryl Bromides with Phenylboronic Acid under Aerobic Conditions. *Eur. J. Inorg. Chem*. 2006, 2642–2646.

65 S. Gao, N. Zhao, M. Shu and S. Che, Palladium nanoparticles supported on MOF-5: A highly active catalyst for a ligand- and copper-free Sonogashira coupling reaction. *Appl. Catal A: Gen*. 2010, **388**, 196-201.

66 A. S. Roy, J. Mondal, B. Banerjee, P. Mondal, A. Bhaumik and S. M. Islam, Pd-grafted porous metal–organic framework material as an efficientand reusable heterogeneous catalyst for C–C couplingreactions in water. *Appl. Catal A: Gen*. 2014, **469**, 320−327.

67 Z. Pahlevanneshan, M. Moghadam, V. Mirkhani, S. Tangestaninejad, I. Mohammadpoor−Baltork and S. Rezaei, Suzuki–Miyaura C–C coupling reactions catalyzed by a homogeneous and nanosilica supported palladium(II) *N*-heterocyclic carbene complex derived from 3,5-di(1-imidazolyl)pyridine. *New J. Chem*. 2015, **39**, 9729-9734.

68 S. Yasar, E. O. Ozcan, N. Gubuz, B. Cetinkaya and I. Ozdemir. Palladium-Catalyzed Heck Coupling Reaction of Aryl Bromides in Aqueous Media Using Tetrahydropyrimidinium Salts as Carbene Ligands. *Molecules*, 2020, **15**, 649−659.

69 W. A. Herrmann and V. P. W. Bohm, Heck reaction catalyzed by phospha-palladacycles in non-aqueous ionic liquids**.** *J. Organomet. Chem*. 1999, **572**. 141−145.

70 K. Okumura, T. Tomiyama, S. Moriyama, A. Nakamichi and M. Niwa, Enhancement in the Catalytic Activity of PD/USY in the Heck Reaction Induced by H_2 Bubbling. *Molecules*, 2011, **16**, 38−51.

71 M. Yigit, G. Bayam, B. Yigit and I. Ozdemir, The Synthesis of 1,3-dialkyl-4-methylimidazolinium Salts and Their Application in Palladium Catalyzed Heck Coupling. *Turkish J. Chem*. 2015, **39**, 281−289.

72 L. Yu, Y. Huang, Z. Wei, Y. Ding, C. Su and Q. Xu, Heck Reactions Catalyzed by Ultrasmall and Uniform Pd Nanoparticles Supported on Polyaniline. J. Org. Chem. 2015, 80, 8677−8683.

73 Y. C. Lin, H. H. Hsueh, S. Kanne, L. K. Chang, F. C. Liu and I. J. B. Lin. Efficient PEPPSI-Themed Palladium N-Heterocylic Carbene Precatalysts for the Mizoroki-Heck Reaction. *Organometallics*, 2013, **32**, 3859-3869.

View Article Online
DOI: 10.1039/C6RA16704G

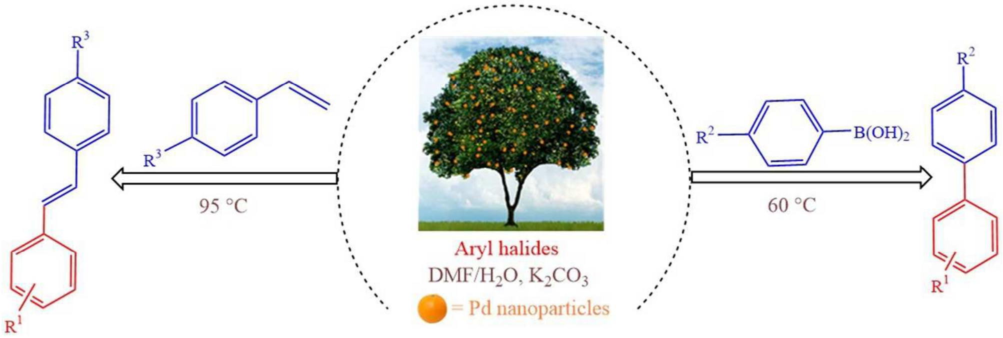

199x66mm (144 x 144 DPI)